Proposal of an InP-based few-mode transmitter based on multimode interference couplers for wavelength division multiplexing and mode division multiplexing applications

Zhaosong Li (李召松)[1], Dan Lu (陆 丹)[1,*], Bing Zuo (左 冰)[2], Song Liang (梁 松)[1], Xuliang Zhou (周旭亮)[1], and Jiaoqing Pan (潘教青)[1]

[1]*Key Laboratory of Semiconductor Materials Science and Beijing Key Laboratory of Low Dimensional Semiconductor Materials and Devices, Institute of Semiconductors, Chinese Academy of Sciences, Beijing 100083, China*

[2]*Network Technology Research Institute, China United Network Communications Corporation Limited, Beijing 100048, China*

**Corresponding author: ludan@semi.ac.cn*

Received March 11, 2016; accepted June 14, 2016; posted online July 11, 2016

An InP-based monolithically integrated few-mode transmitter aiming at the combination of wavelength division multiplexing (WDM) and mode division multiplexing (MDM) technologies is proposed. The core elements of the proposed transmitter are mode converters and a wavelength-mode division multiplexer that are all based on multimode interference (MMI) couplers. Simulations show that the wavelength-mode division multiplexer has a large fabrication tolerance of 30 and 0.5 μm for the length and the width of the device, respectively. A low loss below 0.26 dB for the passive parts of the transmitter is obtained in the whole C-band wavelength range.

OCIS codes: 250.5300, 060.4230, 060.4510.
doi: 10.3788/COL201614.080601.

Mode-division multiplexing (MDM) technology has emerged as an effective solution to increase the fiber capacity in addition to the commonly used technologies, such as wavelength division multiplexing (WDM)[1–3], optical time division multiplexing (OTDM), polarization division multiplexing (PDM)[4,5], and advanced modulation formats. In a typical MDM system, mode conversion and multiplexing are indispensable for the transmitters, where the fundamental laser/fiber mode should be converted to high-order modes and multiplexed into a common output. Many structures have been proposed to realize mode conversion and multiplexing, which typically includes fiber-based technology[6], free-space-optics-based technology[7], and integrated-waveguide-based technology. In terms of functionality and mass-production capability, integrated waveguide technologies are promising due to their capability to be integrated with other devices on chips. Typical structures used in integrated waveguide technologies include directional couplers[8,9], adiabatic couplers[10], and multimode interference (MMI) couplers[11,12]. Due to its large fabrication tolerance and low loss, the MMI-based mode converter-multiplexer will be a potential candidate for integrated few-mode systems. In addition, as a building block for photonic integrated circuit, MMI has been widely adopted in the generic foundry model[13], enabling a high possibility of large scale integrated with active components.

The principle of MMI is based on the self-imaging effect, which can reproduce single or multiple images of the input optical field profile along the propagation of the light[14]. By choosing a proper length, width, and positions of the input and output arms of the MMI, it is possible to realize mode conversion between the fundamental TE_0 mode and the first-order TE_1 mode[15]. Several groups have reported the design and realization of the MMI-based mode converter/(de)multiplexer on silicon on insulator (SOI) substrate[9,11,16]. Thanks to the large wavelength tolerance of the MMI structure, the mode converter/(de)multiplexer can work in a wide wavelength range, which also indicates a possibility of WDM-compatible functionality. Considering the integration possibility of laser sources, modulators, mode converters, and wavelength-mode division multiplexers, an MDM-WDM compatible fully-integrated transmitter would be an attractive solution for future fiber communication systems. It would considerably increase the functionality and decrease the size, power consumption, and cost of such transmitters that may otherwise require a complex combination of discrete components.

In this Letter, we propose an MMI-based few-mode transmitter compatible with WDM technology. The simulation and characterization of the structure was carried out on InP substrate. The device mainly consists of lasers, modulators, and a set of MMIs for mode conversion between the fundamental TE_0 mode and the first-order TE_1 mode for multichannel signals, and one MMI-based wavelength-mode division multiplexer for wavelength and mode multiplexing. The choice of an MMI-based mode converter and multiplexer makes it possible to realize the mode conversion and multiplexing function

through the standard design that is compatible with the generic foundry model. The choice of an InP-based material makes it possible to integrate active components to realize laser generation, modulation, and detection. The intrinsic loss of the MMI-based multiplexer can also be compensated with an optical introduction of semiconductor amplifiers or integrated laser diodes[17].

Figure 1 shows the proposed MMI-based few-mode transmitter on InP substrate. It consists of a series of laser sources, modulators, and MMIs. The laser sources can be distributed feedback (DFB) lasers or distributed Bragg reflector (DBR) lasers. The modulators can be electroabsorption (EA) modulators or Mach–Zehnder modulators. The MMIs function as the power splitters (MMI-1), mode converters/(de)multiplexers (MMI-2), and the wavelength-mode division multiplexer (MMI-3), respectively, with different design parameters. The device is designed to first realize the mode conversion/multiplexing at each wavelength, and then realize wavelength combination for different modes. Take the λ_1 channel as an example, as shown in Fig. 2. The fundamental TE_0 mode from laser diode LD_1 is first split into two branches by a power splitter MMI-1, and then the two fundamental TE_0 modes are independently modulated by modulators Mod-1 and Mod-2. The modulated signals are then sent to a mode converter/multiplexer MMI-2 where one branch of the fundamental TE_0 mode is converted to the first-order TE_1 mode, and combined with another branch of

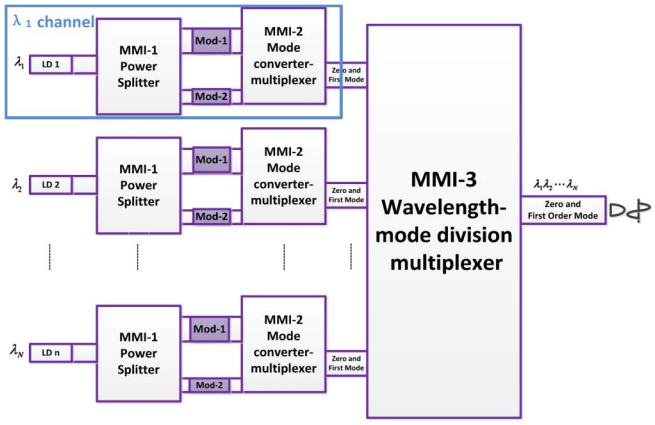

Fig. 1. Schematic diagram of the MMI-based few-mode transmitter.

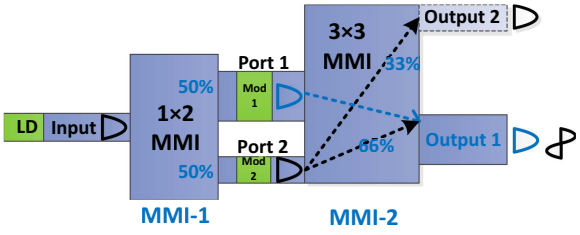

Fig. 2. Schematic diagram of the mode converter/multiplexer.

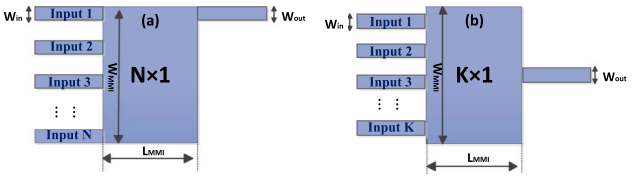

Fig. 3. Schematic diagram of the wavelength-mode division multiplexer: (a) general interference $N \times 1$ MMI and (b) symmetric interference $K \times 1$ MMI.

fundamental TE_0 mode transmitted directly though the MMI-2. Finally, the multiplexed fundamental TE_0 and first-order TE_1 mode at λ_1 are combined with modes from other channels at MMI-3 and sent out from a common port. In this design, MMI-1 is a standard 1×2 MMI splitter, MMI-2 can be structures with 50%, 66%, or 100% mode conversion efficiencies[15], and MMI-3 can be structures of either a general interference $N \times 1$ MMI or a symmetric interference $K \times 1$ MMI, as shown in Fig. 3.

The wavelength-mode division multiplexer MMI-3 is a key component in this design. Even though theoretical results predict that an MMI should be wavelength insensitive in a certain range for an arbitrary input field[18], it is still not clear whether such a structure is suitable for the combination of high-order waveguide modes at multiple wavelengths in terms of engineering manufacturability. So we verified the feasibility of a wavelength-mode division multiplexer using three-dimensional (3D) beam propagation method (BPM) simulations.

For the wavelength-mode division multiplexer MMI-3, the width of the input and output arms are set to be W_{in} and W_{out}, respectively. The width and length of the MMI section are denoted as W_{mmi} and L_{mmi}, respectively. For a general interference $N \times N$ MMI[19], $L_{\text{mmi}} = M/N \times 3L_c$, with $L_c = 4n_{\text{eff}} W_{\text{eq}}^2/3\lambda$, where N represents the number of the in- and outputs, M gives multiples of the shortest MMI having N outputs, L_c represents the coupling length of the fundamental mode and the first-order mode, λ is the wavelength in a vacuum, W_{eq} is the effective width of the MMI taking into account the Goos–Hähnchen shifts, and n_{eff} is the effective refractive index of the ridge. The general MMI can couple any order and number of the inputs into one common output waveguide.

For a symmetric interference $K \times 1$ MMI, $L = 3L_c/2K$, where K is the number of the output waveguides. The symmetric interference MMI can couple odd number of inputs with fundamental TE_0 and first-order TE_1 modes into one common output waveguide.

The epitaxial structure of the InP-based MMI used in the simulation is shown in Fig. 4(a). It consists of a 0.5 μm n-InP buffer, a 0.3 μm InGaAsP core layer with 1.2 μm bandgap (1.2Q), and a 1 μm InP cladding whose effective indexes are 3.167, 3.382, and 3.167, respectively. The cross section view of the waveguides is shown in Fig. 4(b), where an etching depth of 1.15 μm down into the middle of the core layer is adopted to reduce excess loss[20].

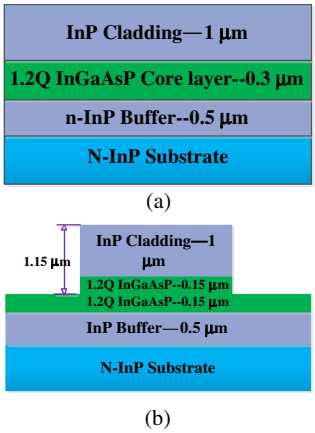

Fig. 4. (a) Epitaxial structure of the MMI, and (b) the cross section view of the waveguide.

Considering the mode matching between the waveguide modes and fiber modes, the fundamental TE_0 and first-order TE_1 waveguide modes are normally the desired mode to be excited and multiplexed. In this case, both the general interference $N \times 1$ and the symmetric interference $K \times 1$ MMIs can be used to function as a multiplexer. To minimize the loss and device size, a $K \times 1$ $(K = 3)$ MMI structure was adopted in the simulation. The width and the length of the symmetric interference 3×1 MMI were set to be 16 and 388 μm, respectively. The width of the input and output waveguides were designed to be 4 μm to support both the fundamental TE_0 mode and the first-order TE_1 mode.

Figures 5(a) and 5(b) show the field distributions when a fundamental TE_0 mode or a first-order TE_1 mode is launched into the input ports of the 3×1 MMI multiplexer, respectively. As can be seen, both the fundamental TE_0 and the first-order TE_1 mode can exit from the common output port, suggesting a mode multiplexing function. Then the wavelength was scanned to verify the wavelength sensitivity of each mode. Figure 6 shows the calculated losses for the TE_0 mode and TE_1 mode, where the intrinsic loss of 4.8 dB for a 3×1 MMI has been subtracted. From the figure, it can be seen that in the whole C-band, the extra losses for the TE_0 mode and TE_1 mode are below 0.2 and 0.8 dB, respectively.

Then the fabrication tolerance was investigated so as to verify the feasibility of such a wavelength-mode division multiplexer. The fabrication tolerance of the MMI's width and length were scanned at different wavelengths for both the TE_0 and TE_1 mode. Figure 7 shows the calculated tolerance of the length and width of the MMI. The fabrication tolerance is defined such that the deviation from the optimum device dimension will result in an extra loss below 3 dB for the two modes. From the simulations, the wavelength-mode division multiplexer was found to have a tolerance of about 30 and 0.5 μm, respectively, for the length and width direction of the MMI in the whole C-band, as shown in Fig. 7.

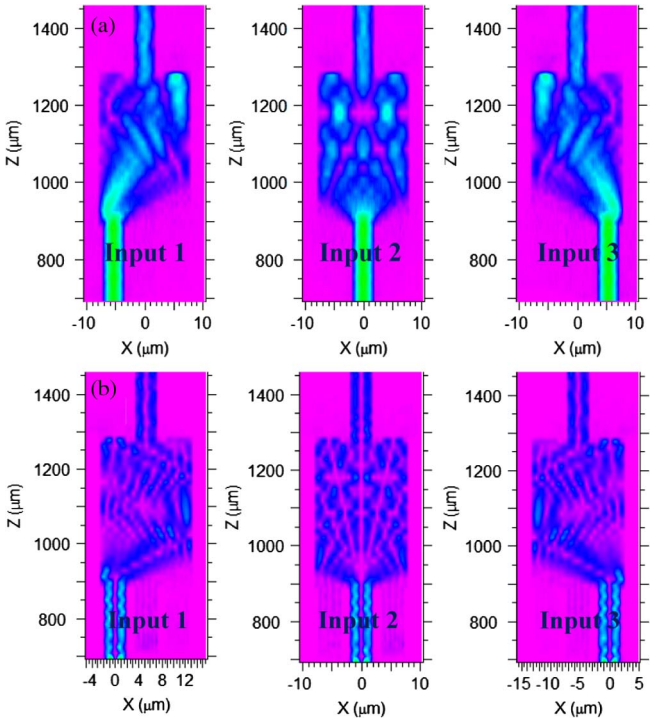

Fig. 5. Field distributions of a 3×1 symmetric interference MMI as a multiplexer (MMI-3) when (a) a fundamental TE_0 mode or (b) a first-order TE_1 mode is injected into a different input port.

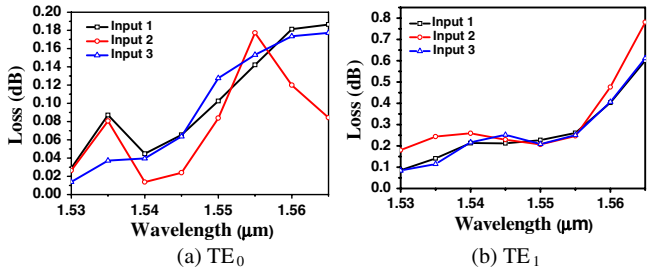

Fig. 6. Wavelength sensitivity of the 3×1 MMI wavelength-mode multiplexer when (a) the fundamental TE_0 modes or (b) the first-order TE_1 modes are launched from port 1 to port 3.

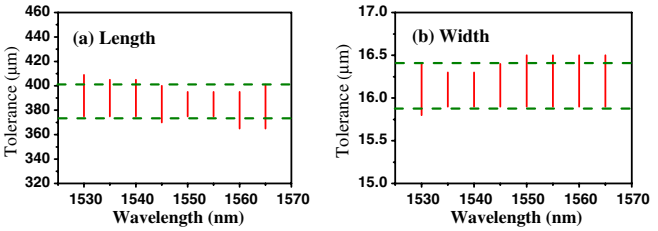

Fig. 7. Simulated fabrication tolerance for the (a) length and (b) width direction of the wavelength-mode division multiplexer.

Then all the contributions of MMI-1, MMI-2, and MMI-3 were calculated. The simulation was divided into two steps. The first step was to calculate the field distribution when a TE_0 mode was transmitted through

MMI-1 and MMI-2. The second step was to send the different modes obtained from step 1 to the wavelength-mode division multiplexer MMI-3. In the simulation, the 1×2 MMI-1 was designed to have a width of 15 μm and a length of 255 μm. MMI-2 was designed to be a 66% mode converter/multiplexer, as a tradeoff between mode conversion efficiency and device size, with a width of 13 μm and a length of 510 μm. The total length of the three MMI sections was 1153 μm. The optical field distributions after the first step are shown in Figs. 8(a)–8(c). Figures 8(a) and 8(b) demonstrate the field distributions when one of the feeding arms connecting to MMI-2 is disconnected, which corresponds to a fundamental TE_0 mode output and a first-order TE_1 mode output, respectively. Figure 8(c) demonstrates the cases when both feeding arms are connected to MMI-2, where a mode-multiplexed pattern combing both the TE_0 and TE_1 mode can be observed in Output 2. The simulated field distributions after MMI-3 are shown in Figs. 8(d)–8(f) to demonstrate the cases when the multiplexed modes obtained in Output 2 are incident to the three input ports of the MMI-3, respectively. The simulated loss of the whole passive parts (MMI-1, MMI-2, and MMI-3) in the transmitter shows a maximum loss of below 0.26 dB (after subtracting the intrinsic loss of the MMIs) in the C-band, as shown in Fig. 9.

To realize the mode conversion/multiplexing of the high-order modes, the 66% mode converter/multiplexer (MMI-2) can be replaced by other designs like[21]. The wavelength-mode multiplexer (MMI-3) can also be

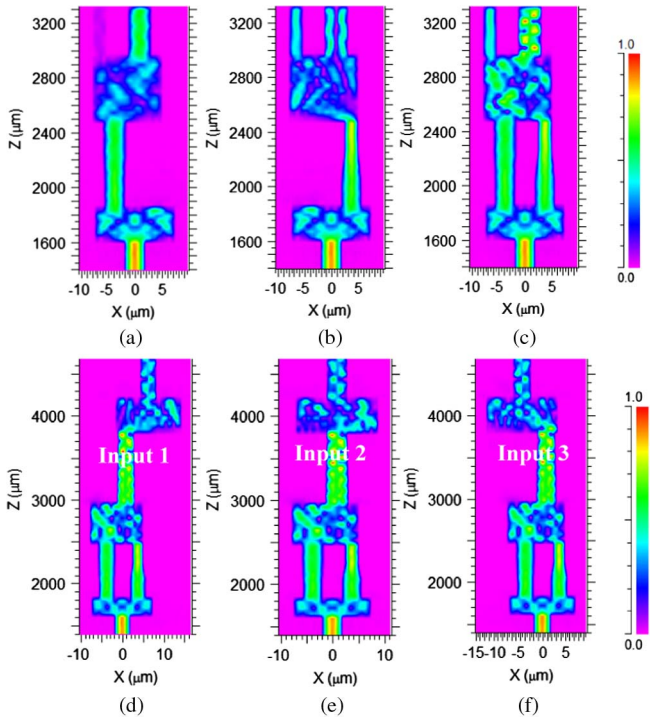

Fig. 8. Field distribution when an input TE_0 mode transmits through (a–c) MMI-1 and MMI-2 and (d–e) MMI-1, MMI-2, and MMI-3. (a) and (b) are obtained by disconnecting one of the feeding arms to MMI-2.

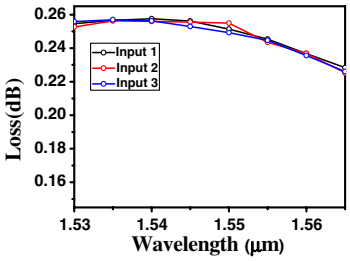

Fig. 9. Simulated loss vs. wavelength for the whole device (the intrinsic loss of MMIs has been subtracted).

replaced easily by the other symmetric interference $K \times 1$ MMI couplers (K being an odd number) or general interference $N \times 1$ MMI couplers (N being a positive integer) when the wavelength channel increases, where K and N are the number of the output waveguides.

For such an integrated device, the back reflection from the MMI couplers may influence the dynamics of the lasers, since there are no conventional isolators placed between the lasers and the MMIs. The major contribution comes from the reflection from the self-imaging point where there is no output port in which case the light at the self-image point will be reflected back into the input port and further back into the laser. A typical example is Output 2 of MMI-2, as shown in Fig. 2. When there is no actual output waveguide at Output 2, the reflectivity between the InP/InGaAsP materials and the air is about 0.3. Assuming the laser has a confinement factor of 0.05, the fraction of the laser power coupled into the laser active region will be on the order of 0.1% (−30 dB) after a simple arithmetic calculation. Such a back reflection level might destabilize the laser depending on the specific laser structure and material. The problem can be easily solved by introducing an absorption section at the position of Output 2. For reflections from the output ports of MMI-3, antireflection coating with a reflectivity below 1% will guarantee a feedback level well below −50 dB, which can hardly destabilize the laser. Other contributions from the interface reflections between the access waveguide and the MMIs are calculated to be lower than −70 dB, which can be omitted here. In real applications, MMIs with angled, rough, or absorbing end facets also can be adopted to minimize the influence of the end reflection.

In conclusion, an InP-based monolithically integrated few-mode transmitter aiming at the combination of WDM and MDM technologies is proposed by using cascaded MMI couplers. The core element of the transmitter is an MMI-based wavelength-mode division multiplexer. The performance and manufacture tolerance of the wavelength-mode division multiplexer was simulated through the 3D BPM method. Simulations show that such a multiplexer has a large fabrication tolerance of 30 and 0.5 μm, respectively, in the length and width direction, in the whole C-band wavelength range. The loss is below 0.26 dB for both the fundamental TE_0 mode and first-order TE_1 mode in the whole passive parts of the transmitter. This

wavelength-mode division multiplexer can be integrated with other active components, capable of realizing a few-mode transmitter with WDM functionality.

This work was supported by the National 973 Program of China (No. 2014CB340102) and the National Nature Science Foundation of China (Nos. 61320106013 and 61271066).

References

1. G.-K. Chang, A. Chowdhury, Z. Jia, H.-C. Chien, M.-F. Huang, and J. Yu, J. Opt. Commun. Netw. **1**, C35 (2009).
2. Z. Zhang, X. Jiang, J. Wang, X. Chen, and L. Wang, Chin. Opt. Lett. **13**, 020603 (2015).
3. O. Ozolins and V. Bobrovs, Chin. Opt. Lett. **13**, 060603 (2015).
4. L. Han, S. Liang, H. Zhu, C. Zhang, and W. Wang, IEEE Photon. Technol. Lett. **27**, 782 (2015).
5. A. H. Gnauck, G. Charlet, P. Tran, P. J. Winzer, C. R. Doerr, J. C. Centanni, E. C. Burrows, T. Kawanishi, T. Sakamoto, and K. Higuma, J. Lightwave Technol. **26**, 79 (2008).
6. P. Sillard, M. Bigot-Astruc, and D. Molin, J. Lightwave Technol. **32**, 2824 (2014).
7. E. Ip, N. Bai, Y. Huang, E. Mateo, F. Yaman, M. Li, and S. Bickham, in *37th European Conference on Optical Communication* **1**, Th.13. C.2 (IEEE, 2011).
8. Y. De Yang, Y. Li, Y. Z. Huang, and A. W. Poon, Opt. Express **22**, 22172 (2014).
9. T. Mulugeta and M. Rasras, Opt. Express **23**, 943 (2015).
10. J. Xing, Z. Li, X. Xiao, J. Yu, and Y. Yu, Opt. Lett. **38**, 3468 (2013).
11. Y. Chaen, R. Tanaka, and K. Hamamoto, in *Microoptics Conference*, pp. 2 (2013).
12. L. Han, S. Liang, H. Zhu, L. Qiao, J. Xu, and W. Wang, Opt. Lett. **40**, 518 (2015).
13. M. Wale, J. Van der Tol, X. Leijtens, N. Grote, H. Ambrosius, M. Schell, D. Robbins, M. Smit, and E. Bente, IET Optoelectron. **5**, 187 (2011).
14. O. Bryngdahl, J. Opt. Soc. Am. **63**, 416 (1973).
15. J. Leuthold, J. Eckner, E. Gamper, P. A. Besse, and H. Melchior, J. Lightwave Technol. **16**, 1228 (1998).
16. L. W. Luo, N. Ophir, C. P. Chen, L. H. Gabrielli, C. B. Poitras, K. Bergmen, and M. Lipson, Nat. Commun. **5**, 1 (2014).
17. M. Yanagisawa, T. Hashimoto, F. Ebisawa, T. Kitagawa, H. Ttakahashi, A. Himeno, A. Sugita, Y. Yamada, and K. Okamoto, in *24th European Conference on Optical Communication*, Vol. **1**, p. 77 (IEEE, 1998).
18. M. Bachmann, P. A. Besse, and H. Melchior, Appl. Opt. **33**, 3905 (1994).
19. R. M. Jenkins, R. W. J. Devereux, and J. M. Heaton, Opt. Lett. **17**, 991 (1992).
20. F. Guo, D. Lu, R. Zhang, B. Wang, X. Zhang, and C. Ji, J. Semicond. **35**, 024012 (2014).
21. J. Qiu, D. Zhang, Y. Tian, J. Wu, Y. Li, and Y. Wang, IEEE Photonics J. **7**, 1 (2015).